Available online at www.sciencedirect.com
SCIENCE DIRECT
Corrosion Science 48 (2006) 2154–2171
CORROSION SCIENCE
www.elsevier.com/locate/corsci

Corrosion behaviour of magnetron sputtered α- and β-Ta coatings on AISI 4340 steel as a function of coating thickness

S. Maeng [a,*], L. Axe [a], T.A. Tyson [b], L. Gladczuk [c], M. Sosnowski [c]

[a] *Department of Civil and Environmental Engineering, New Jersey Institute of Technology, University Heights, Newark, NJ 07102, USA*
[b] *Department of Physics, New Jersey Institute of Technology, Newark, NJ 07102, USA*
[c] *Department of Electrical and Computer Engineering, New Jersey Institute of Technology, Newark, NJ 07102, USA*

Received 20 December 2004; accepted 9 August 2005
Available online 27 September 2005

Abstract

The corrosion behaviour of magnetron sputtered α- and β-Ta coated AISI 4340 steels was studied with potentiodynamic polarization and electrochemical impedance spectroscopy. The coating porosity was observed to decrease with increasing coating thickness. For coatings less than 10 μm thick (α- or β-Ta), porosity was significant and open pores resulted in severe localized corrosion of the steel substrate, coating delamination, and overall coating failure. Additionally, the β-Ta coatings were more susceptible than the α-phase to delamination. As for the 50 and 100 μm thick α-Ta coatings, the electrochemical impedance behaviour was comparable to that of Ta foil, demonstrating the coating viability and corrosion resistance.

Keywords: A. Tantalum; B. Magnetron sputtering; C. Coating thickness; C. Corrosion behaviour

1. Introduction

Tantalum coatings produced by physical vapor deposition (PVD) have been investigated as a replacement for Cr coatings to protect gun-bore from erosion and corrosion

* Corresponding author. Tel.: +1 973 596 6077; fax: +1 973 596 5790.
E-mail address: smm8166@njit.edu (S. Maeng).

0010-938X/$ - see front matter
doi:10.1016/j.corsci.2005.08.007

[1,2]. Bulk Ta (α phase) shows excellent physical and chemical properties such as a high melting point (2996 °C), good ductility, and excellent corrosion resistance in aggressive environments. However, under varying deposition conditions, α-Ta (body-centered cubic structure), β-Ta (tetragonal structure), or a mixture of both phases have been observed [3,4]. In contrast to the tough and ductile α-Ta phase, β-Ta phase is hard and brittle, and its presence compromises the coating integrity under strain. Therefore, the α phase is preferred in application where coatings are subjected to both chemical attack and wear, such as protecting gun-bore against erosion.

A metal coating deposited without impurities or defects should exhibit corrosion behaviour comparable to that of the bulk metal. However, in practice it is generally not feasible to achieve such coatings, especially thin ones. Consequently, the potential presence of defects (i.e., pinhole, open pores) in coatings may result in severe localized corrosion due to the galvanic action when the coating is cathodic with respect to the substrate [5]. This galvanic effect, localized at open pores, is increased by an unfavorable surface ratio, when the cathodic area is much greater than the anodic area. One method to minimize the presence of defects penetrating the coating from the surface to the substrate is to increase the coating thickness. Coating porosity is in general inversely proportional to coating thickness; this reduction has been observed to occur for the most part irrespective of the coating process [5]. Therefore, it is critical to obtain a minimum thickness for defect-free coatings, which have corrosion performance similar to that of the bulk metal.

Electrochemical techniques including DC corrosion and electrochemical impedance spectroscopy (EIS) have been employed to evaluate the corrosion behaviour and porosity of metallic and ceramic coatings [6–11]. For example, Elsener et al. [6] evaluated porosity of PVD and chemical vapor deposition (CVD) TiN coated steel at the free corroding potential. Assuming that the coating is electrochemically inert at the open circuit potential the authors estimated the porosity from polarization resistance and reported that the PVD coatings were 25 times less porous than the CVD ones. However, both coatings on mild steel showed severe localized corrosion at film defects. In addition, Liu et al. [11] compared the degree of delamination of TiN and CrN coatings as a function of time and found delamination was greater for the TiN coating than for the CrN one. Their study demonstrated that, as immersion time increased, galvanic corrosion became localized at open pores where steel substrate dissolution occurred, causing delamination of the adjacent coating.

In our study, α-Ta and β-Ta coatings with thicknesses of 5 μm, 10 μm, 50 μm, and 100 μm deposited on AISI 4340 steel using DC magnetron sputtering were investigated with potentiodynamic polarization and EIS. Morphological evaluation of the surface and cross-sections after corrosion tests was conducted using scanning electron microscopy (SEM). In addition, galvanic corrosion behaviour of Ta and steel substrate was studied by varying the area ratio of Ta to the steel substrate.

2. Experimental details

2.1. Preparation of substrates and Ta deposition

The substrates machined from AISI 4340 steel had the form of square coupons, 12.6 mm × 12.6 mm, 6 mm thick. Before loading, the substrate was electrochemically

cleaned and mechanically polished with diamond suspensions of decreasing particle size, down to 0.05 μm. The polished steel substrates were then cleaned ultrasonically in acetone and methanol. The surface roughness of the polished steel substrates measured by AFM was 12.4 ± 1.9 nm (rms).

Tantalum was deposited by DC magnetron sputtering in argon gas (99.995% purity) at a pressure of 0.7 Pa [12]. The base pressure in the process chamber was 1.1×10^{-5} Pa. A tantalum target (99.95%) with a 50 mm diameter was mounted 50 mm below the substrate holder. After loading into the chamber, the substrates were baked in vacuum at 200 °C by an internal halogen lamp for at least 6 h. Prior to deposition, the substrates were sputter-etched for 10 min with Ar at a pressure of 30 Pa and a DC bias of −400 V.

The α-Ta coatings of 5, 10, 50, and 100 μm and β-Ta coatings of 5 and 10 μm were produced within 20% variation of the desired thickness; production of thicker coatings of the β-phase were not possible due to its metastability. A deposition rate of 1.2 nm/s with the source current of 0.5 A and a target voltage of −300 V was used for the 5 and 10 μm coatings. For thicker coatings, the initial deposition rate was 1.2 nm/s, up to 3 μm thickness, and then the source current was increased to 1 A with a target voltage of −375 V, resulting in a deposition rate of 2.4 nm/s. The substrates were at the ground potential. Without intentional substrate heating, depositions produced β-Ta coatings. Temperatures of the substrate, measured by a thermocouple, were below 100 °C for all deposition rates. To produce the α-phase, the steel temperature during deposition was held at approximately 420 °C, using a substrate heater. Details of the apparatus and the deposition procedure are given elsewhere [12]. Polished Ta foils (99.9%) and polished steel substrates (AISI 4340) were used as references for electrochemical tests.

2.2. Coating characterization

To identify the crystallographic phase of the deposited coatings X-ray diffraction (XRD) was performed using a Philips X-ray diffractometer (Bragg–Brentano θ:θ) with CuKα radiation operated at 45 kV and 40 mA. To measure microscopic roughness of the coatings atomic force microscopy (Nanoscope IIIA Multimode scanning probe microscope, Digital Instruments) was employed in contact mode. Before and after the corrosion tests, the surface and corrosion features of coated samples were examined using a field emission scanning electron microscope (FE-SEM, LEO 1530) and capable of qualitative elemental analysis by energy dispersive X-ray spectroscopy (EDX, Oxford INCA Energy 400). The corrosion products could therefore be qualitatively assessed at the pinhole defects.

2.3. Electrochemical tests

The test solution for electrochemical investigations was a deaerated 0.5 M H_2SO_4, which was prepared by diluting the standardized 10 N H_2SO_4 (ACS reagent grade) with deionized water and purging with N_2 gas (99.999% purity) at a rate of 1.0 L/min for 1 h before an electrochemical test. The solution was also continuously purged with the N_2 gas at a rate of 0.5 L/min during the experiment. All studies were conducted at room temperature (22 ± 3 °C).

2.3.1. Galvanic current measurement

Tantalum is an electrochemically active metal as its thermodynamic nobility lies below zinc. However, once passivated, its stable oxide film places tantalum above gold in practical nobility [13]. Therefore, Ta has the tendency to be cathodic to steel when exposed to an electrolyte through open pores. To assess the galvanic behaviour of the Ta and steel (AISI 4340) couple, galvanic currents with cathodic (Ta foil) to anodic (AISI 4340 steel) area ratios of 0.82, 3.4 and 11.33 were measured using a zero resistance ammeter during a total immersion time of 24 h.

2.3.2. Potentiodynamic polarization and EIS

Potentiodynamic polarization and EIS measurements were carried out using a Gamry PC4/300 computerized system for collecting and analyzing electrochemical data. A Flat cell (Princeton Applied Research) was used with a three-electrode configuration including a saturated calomel electrode (SCE) and platinum gauze as reference and auxiliary electrodes, respectively. All electrochemical corrosion tests were carried out with an exposure area of 1 cm^2.

Potentiodynamic polarization was measured 1 h after immersion with a scan rate of 10 mV/min from −0.2 to +1.5 V versus the open circuit potential (OCP). EIS data were collected at OCP with a sinusoidal voltage perturbation of 10 mV (rms) over the frequency range of 10 mHz to 100 kHz with 7–10 points per decade; these spectra were obtained over 0.5, 1, 4, 8, 24, 48, 72, and 96 h of exposure time. The data were analyzed using complex nonlinear least squares fitting (CNLS) LEVM algorithm [14] in the Gamry Echem Analyst software.

3. Results and discussions

3.1. Phase and microstructure of Ta coatings

The thin α-Ta coatings of 5 and 10 μm show (1 1 0) preferred orientation (Fig. 1), while thicker α-Ta coatings show (2 2 2) preferred orientation; presence of β-phase was not observed in these coatings. For the β-Ta coatings three peaks (Fig. 1), referred to as (0 0 2), (0 0 4), and (0 0 6) are observed with no trace of the α-phase. In general, β-Ta films exhibit (0 0 2) texture [15]. Bulk Ta foil shows a slightly preferred (1 1 0) orientation with a very similar pattern to that of Ta powder. Interestingly, mechanical polishing changed the foil orientation to the (2 2 2) reflection.

Thin α-Ta coatings were relatively smooth with the rms roughness (R_{rms}) of 5 μm and 10 μm coatings measured at 5.6 nm and 9.8 nm, respectively. The roughness clearly increased with coating thickness and was significantly greater for 50 μm ($R_{rms} = 29.3$ nm) and 100 μm ($R_{rms} = 22.1$ nm) α-Ta coatings. Thin β-Ta coatings had similar roughness ($R_{rms} = 7.2$ and 9.2 nm for 5 and 10 μm thickness, respectively) to that of thin α-Ta coatings but exhibited somewhat finer surface features. As discussed earlier, 50 and 100 μm Ta coatings were deposited at a higher sputtering rate, which (not unexpectedly) appears to increase the surface roughness as compared to the slower process. SEM imaging of the coatings surface morphology showed uniform coverage of the steel substrate area without any cracks. However, the presence of some defects such as pinhole and droplet-like clusters that are commonly found in PVD processes [11,16,17] is observed on the coated surface regardless of thickness and phase (α and β). Pinholes are observed only on the surface

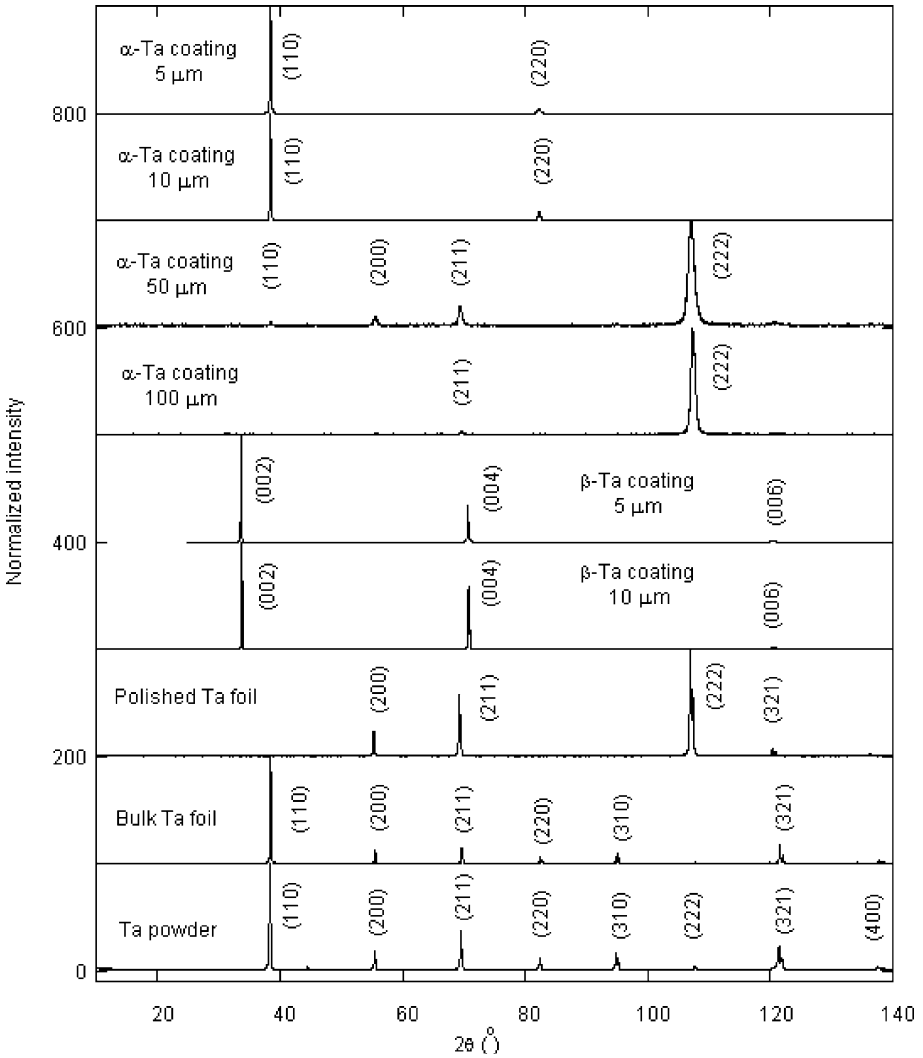

Fig. 1. X-ray diffraction patterns of α- and β-Ta coatings, Ta foil (polished and unpolished) and Ta powder. XRD patterns are normalized with respect to the peak with maximum intensity in each spectrum.

of thin coatings, while the droplet shape defects are seen on both thin and thick coatings (Fig. 2a). The formation of pinholes is relatively rare, compared to droplet-like defects. The distribution of droplet-like defects appears to be random and their density is reduced as the coating thickness increases. Defects in the form of open pores or voids extending from the coating surface to the substrate are of most concern as they provide a channel for electrolyte penetration to the steel and hence, initiate localized corrosion, enhanced by the galvanic effect. SEM image of a droplet-like defect in a thin Ta coating on steel, after the potentiodynamic polarization test, is shown in Fig. 2b. The results of EDX measurements indicate the presence of Fe, O and S elements related to the corrosion products. These results reveal that corrosion of the steel substrate covered with thin α- and β-Ta

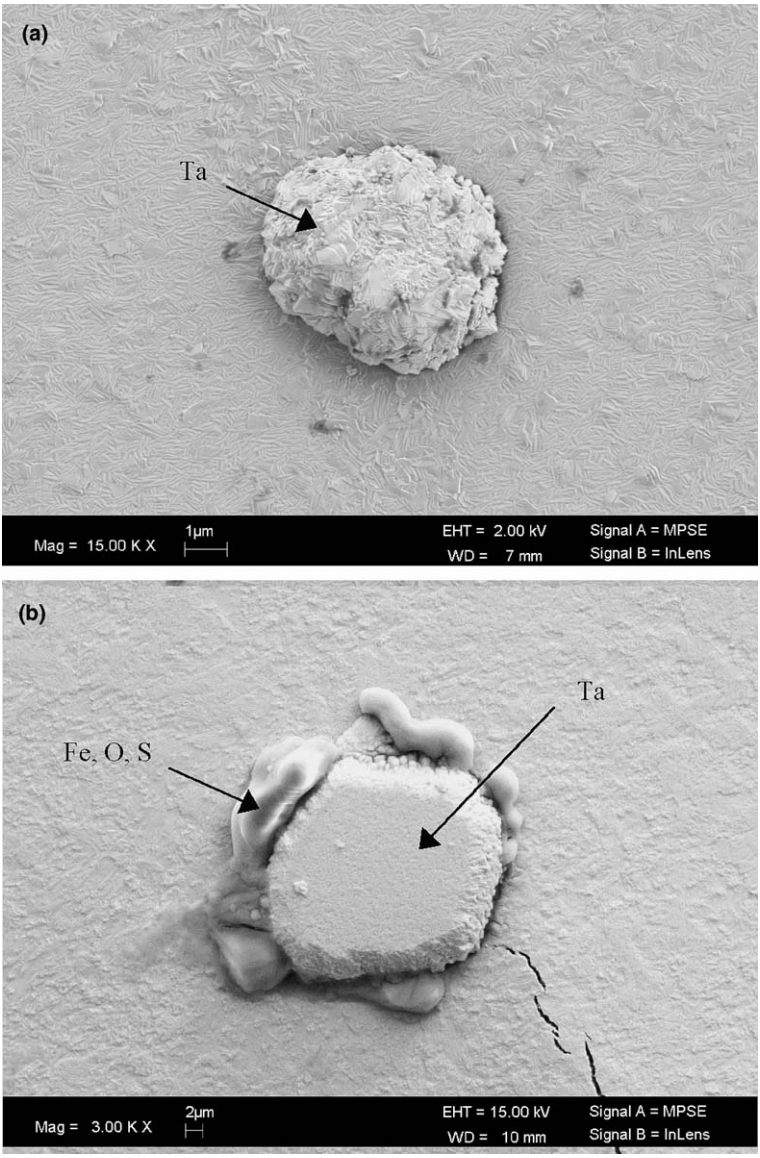

Fig. 2. Typical SEM images of Ta coating showing (a) a droplet-like defect before corrosion and (b) the corrosion of the steel substrate through defects and propagation of cracks initiated from defects after potentiodynamic polarization measurements.

coatings occurs through defects. There was no evidence of steel substrate dissolution for the 50 and 100 μm thick coatings. Therefore, defects such as pinholes and porosity are major factors and the overall corrosion process appears to be dominated by locally active substrate dissolution through open pores. Porosity evaluation is thus critical for the quality control of the coatings.

3.2. Galvanic corrosion

To evaluate the galvanic corrosion effect between Ta and steel (AISI 4340) substrate, the evolution of the galvanic current was measured as a function of the surface area ratio of cathode (Ta foil) to anode (AISI 4340 steel) (0.82:1 to 11.33:1). During the measurement, the galvanic current density (i_g) was constant and no reversal in polarity was observed, indicating that the surface conditions for both electrodes appear to be stable. The current density was observed to increase linearly ($r^2 = 0.98$) as the cathode to anode areas ratio increased (Fig. 3). Nevertheless, the magnitude of the current density ($\approx 5.48 \times 10^{-4}$ mA/cm^2 for a surface area ratio of 11.33) was much smaller than the corrosion current density of the steel substrate (≈ 0.558 mA/cm^2). Additionally, the galvanic potential measured in Ta/steel coupling was close to the open circuit potential of the steel (-454 mV versus SCE). These results demonstrate that the galvanic current density is not equivalent to the steel dissolution rate when the anode is polarized slightly from its corrosion potential [18]. In Ta/steel coupling, the contribution of cathodic reduction of H^+ to the dissolution of steel appears to be insignificant.

When the steel substrate is exposed to electrolyte through open micropores in the Ta coating localized corrosion is accelerated due to the galvanic action. To better understand the relationship between porosity, open pores, and coating viability, measurements of potentiodynamic polarization were conducted.

3.3. Potentiodynamic polarization

The polarization curves of the Ta coatings of different thickness, Ta foil, and AISI 4340 steel were obtained 1 h after immersion (Fig. 4). The corrosion and passivation current

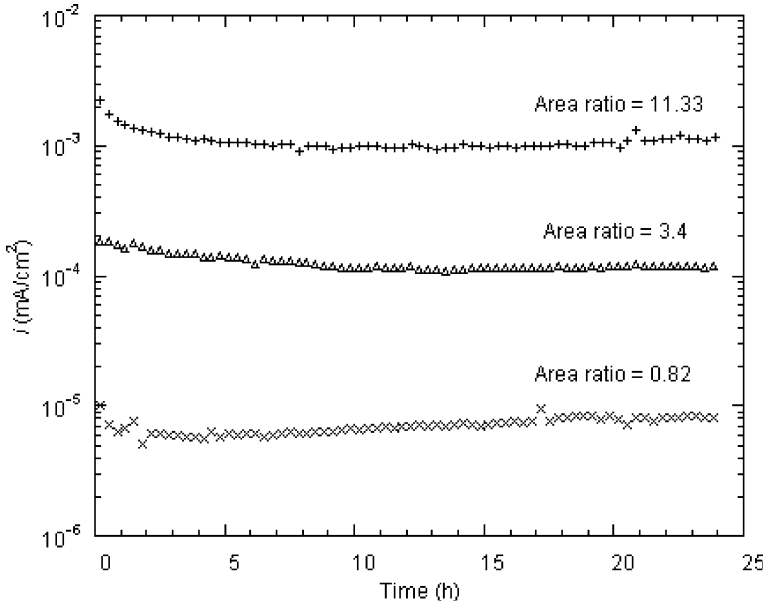

Fig. 3. Evolution of galvanic current density measured with different ratios of cathodic (Ta foil) to anodic (AISI 4340 steel) areas in deaerated 0.5 M H_2SO_4 with N_2 at room temperature during 24 h.

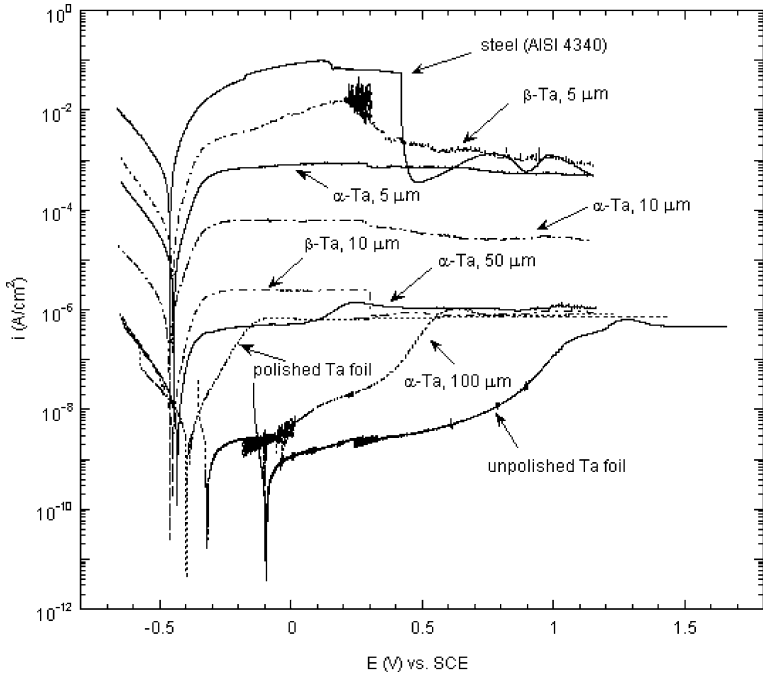

Fig. 4. Anodic polarization curves of α- and β-Ta coatings with different thicknesses, Ta foil, and steel substrate (AISI 4340) in deaerated 0.5 M H_2SO_4 purged with N_2 at room temperature.

densities of α- and β-Ta coatings decreased with increasing coating thickness. For 50 and 100 μm, the corrosion resistance is comparable with that of a polished Ta foil. The latter exhibits almost the same behaviour to that of the unpolished Ta foil, except for the open circuit potential difference (Table 1). Moreover, the polarization resistance of the 100 μm coating falls between that of the unpolished and polished Ta foil; therefore, this coating produced in our PVD system behaves like that of bulk Ta foil with respect to corrosion performance.

The polarization measurements on α-Ta foils showed that the corrosion potential of unpolished Ta foil is greater than that of polished Ta foil and that the polarization resistance of unpolished Ta foil at the corrosion potential is approximately one order of magnitude greater than that of polished Ta foil (Table 1). The polarization resistance of the polished foil is still very high. The difference in the polarization resistances may be due to the difference in thickness or composition of the native oxide film present on the surface of the foils [19].

As the polarization resistance of Ta foil at open circuit potential is five to six orders of magnitude greater than that of AISI 4340 steel (Table 1), the Ta coating is chemically inert and hence, the polarization resistance of Ta coatings measured at open circuit potential is represented by the polarization resistance of the steel substrate exposed to the electrolyte through open pores. In addition, the corrosion potential of Ta coatings less than 100 μm thick is slightly shifted from that of the bare steel substrate and far below its passivation potential, indicating the steel substrate was actively dissolving. In this case, the total

Table 1
Electrochemical characteristics of Ta coatings, Ta foil and steel (AISI 4340) substrate

Thickness (μm)	α-Ta coating/steel (AISI 4340)				β-Ta/steel (AISO 4340)		Ta foil		Steel (AISI 4340)
	5	10	50	100	5	10	Nonpolished	Polished	Polished
E_{corr} (mV versus SCE)	−444	−461	−433	−318	−445	−450	-58 ± 159	-388 ± 44	-454 ± 9
R_p (Ω cm^2)	1.60×10^3	2.27×10^4	1.09×10^6	1.67×10^7	4.58×10^2	7.54×10^5	$3.14 \times 10^7 \pm 1.98 \times 10^6$	$3.14 \times 10^6 \pm 1.29 \times 10^6$	23.8 ± 8.1
b_a (mV/decade)									47.7 ± 2.3

Table 2
The porosity of α- and β-Ta coated steel (AISI 4340) as a function of thickness evaluated from polarization resistance 1 h after immersion

Thickness (μm)	α-Ta coating/steel (AISI 4340)				β-Ta/steel (AISI 4340)	
	5	10	50	100	5	10
P (%)[a]	0.94 ± 0.12	0.073 ± 0.047	0.00079 ± 0.00013	$2.0 \times 10^{-7} \pm 8.8 \times 10^{-8}$	3.8 ± 0.76	0.0026 ± 0.00068

[a] E_{corr}, R_{ps} and b_a of AISI 4340 steel for porosity estimation were −454 mV (versus SCE), 23.8 Ω cm^2, and 47.7 mV/decade, respectively. The error in P is estimated based on the variation in E_{corr}, R_{ps}, and b_a of AISI 4340 steel shown in Table 1.

coating porosity index P, which represents the area ratio of total pores to total exposed surface is estimated using the following equation [6]:

$$P = \left(\frac{R_{p,bs}}{R_p}\right) \times 10^{|\Delta E_{corr}|/b_a} \quad (1)$$

where R_p and $R_{p,bs}$ are the polarization resistances of the Ta coated steel and bare steel substrate, respectively, ΔE_{corr} is the difference in the corrosion potential between the Ta coating and the bare steel substrate, and b_a is the anodic Tafel slope of the bare steel substrate. Increasing coating thickness reduced porosity (Table 2), which is attributed to a void masking effect, i.e., covering the voids (closing pores) by the depositing material. Such a mechanism is effective in coatings with thickness significantly greater than the void size. The effect appears to be more pronounced for thin β-Ta coatings than for α-Ta coatings (in 5–10 μm range), probably due to the finer grain structure of β-Ta.

Using Eq. (1) without a calibration procedure may not provide a highly accurate porosity index value for submicroscopic pores because the equation is dependent on the corrosion resistance of the coating. For example, for polished Ta foil with a R_p of $3.14 \times 10^6\ \Omega$ the equation gives an apparent porosity, 3.1×10^{-5}%, which is greater than that for the 100 μm coating, 2.0×10^{-7}%. Both numbers are insignificant and clearly represent the absence of open pores.

The corrosion resistance of a coating in general varies with increasing immersion time due to potential delamination of the coating and/or blocking of pores by corrosion product [11,20,21]. Therefore, the stability of the Ta coating as a function of immersion time was investigated using EIS.

3.4. Corrosion behaviour as a function of immersion time evaluated by EIS

The impedance spectra, which were collected over 4 days at the corrosion potential, are compared to that of the Ta foil and AISI 4340 steel (Fig. 5a). The impedance at the low frequency plateau in the Bode plot is indicative of the sum of the polarization and the electrolyte resistance; the latter of which is seen at the high frequency plateau. The impedance of Ta foil appears to be at least five orders of magnitude greater than that of AISI 4340 steel, and is in good agreement with that observed in potentiodynamic polarization measurements. Tantalum shows consistent and stable impedance behaviour as a function of exposure time. This stability and large impedance may be attributed to the very stable tantalum oxide film. In addition, the maximum phase angle for Ta foil over all immersion times is close to $\pi/2$, indicative of ideal capacitor behaviour [20] throughout the 4 day exposure. This capacitive behaviour has been reported to be due to the passive film as well as the electrical double layer [19].

The impedance spectra of α-Ta coatings, 50 μm and 100 μm thick, reveal that there was no significant change over 4 days of exposure (Fig. 5b). The phase angle response is very similar to that of Ta foil. In addition only one relaxation time constant in the EIS spectra is observed, as in the case of Ta foil. Therefore, with respect to corrosion performance, the α-Ta coating with a thickness greater than or equal to 50 μm appears to behave in a similar manner to that of Ta foil over long exposure times.

In contrast to thick Ta coatings, the impedance of the thin Ta coatings decreases with increasing immersion time (Fig. 6). This continuous impedance reduction for the thinner coatings can be explained by the steel substrate corrosion through open pores. Localized

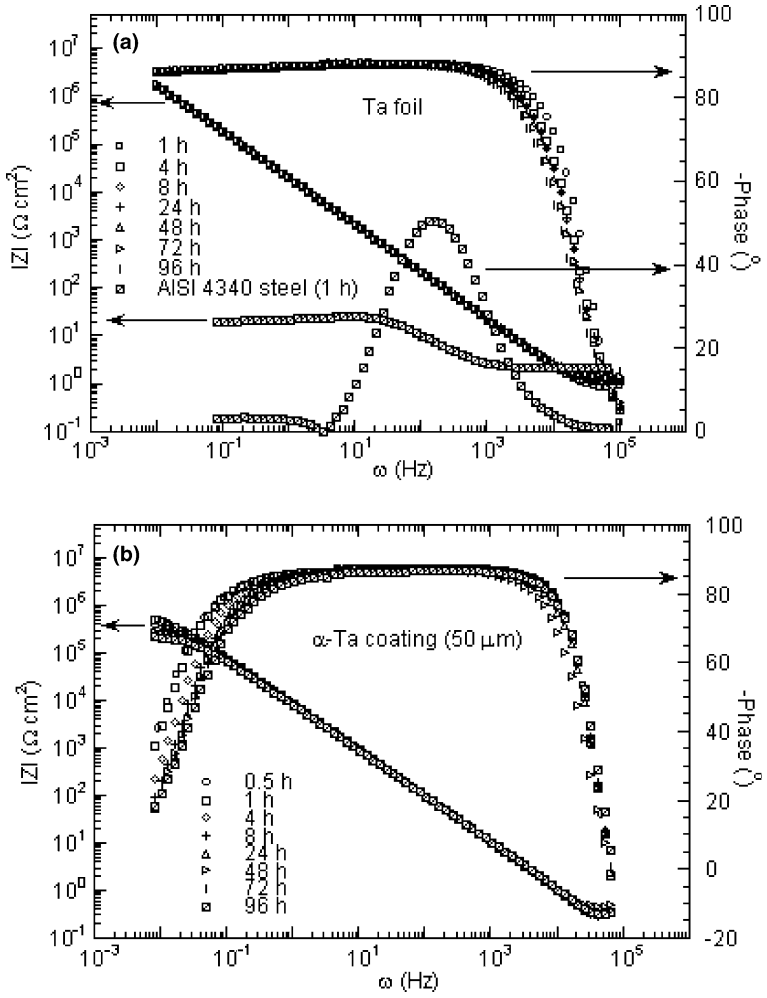

Fig. 5. Impedance spectra of (a) Ta foil after different immersion times and AISI 4340 steel for 1 h exposure and (b) 50 μm α-Ta coating after different immersion times in deaerated 0.5 M H_2SO_4 purged with N_2 at room temperature.

corrosion and delamination of the coating increase in the exposed area of steel substrate with time. While the impedance of the thin α-Ta coatings shows a gradual decrease, the impedance of the thin β-Ta coatings decreases only slightly up to 24 h and then falls dramatically to approach that of AISI 4340 steel. Accordingly, the degree of delamination was greater for β-Ta coatings than for α-Ta ones over the same immersion time. Although some cracks and pinholes were observed in thin α-Ta coatings, β-Ta coatings were cracked around defects and delaminated by the end of experiment (Fig. 7). The greater degree of delamination of β-Ta coatings may be related to their mechanical properties. A section of the hard and brittle coating may initially withstand local stress caused by corrosion but then fails catastrophically exhibiting cracks and delamination. This mode of failure of β-Ta coatings, contrasting ductile behaviour of α-Ta coatings, under mechanical stress

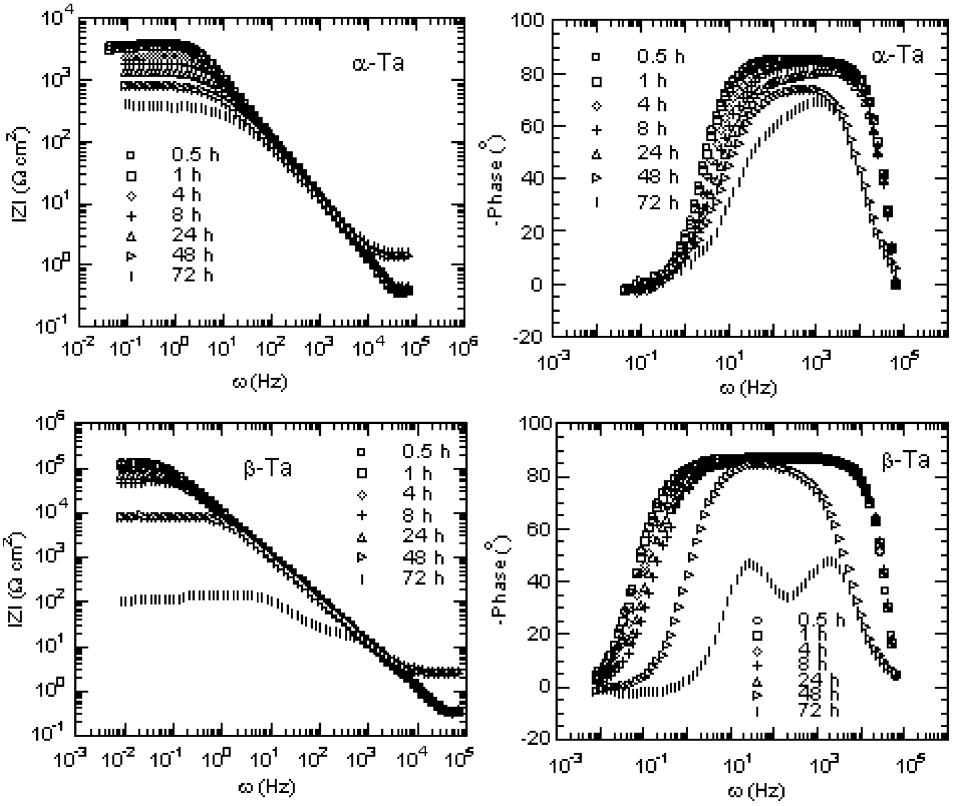

Fig. 6. Typical impedance spectra of thin α- and β-Ta coatings (10 μm thickness) after different immersion times in deaerated 0.5 M H_2SO_4 purged with N_2 at room temperature.

has been demonstrated recently [12]. Nevertheless, the cross-sectional SEM images (Fig. 7) show severe localized corrosion of the steel substrates under both thin α- and β-Ta coatings.

The initial phase angle responses of the thin Ta coatings (Fig. 6), however, are very similar to that of Ta foil (Fig. 5a), reflecting capacitive behaviour, which is not representative of steel substrate corrosion through open pores. However, as exposure time increases, the development of two time constants becomes evident. The short relaxation time constant, associated with a high-frequency process is related to the coating/solution interface and the dielectric characteristic of the native oxide film, whereas the low-frequency process is related to the substrate/solution interface at the open pores and represents corrosion of the steel substrate.

To analyze the impedance spectra, two equivalent circuit (EC) models are proposed, as shown schematically in Fig. 8. The EC model in Fig. 8a has been used for describing the impedance spectra of Ta/Ta oxide/electrolyte structure [19,22]. Kerrec et al. [19] reported that a constant phase element (cpe) behaviour, indicative of capacitance dispersion, is attributable to heterogeneities in the tantalum oxide composition. As thick α-Ta coatings (Fig. 5b) showed very similar impedance behaviour to that of Ta foil (Fig. 5a), the EC shown in Fig. 8a was used to fit the EIS data. Here, R_p for Ta foil represents the polari-

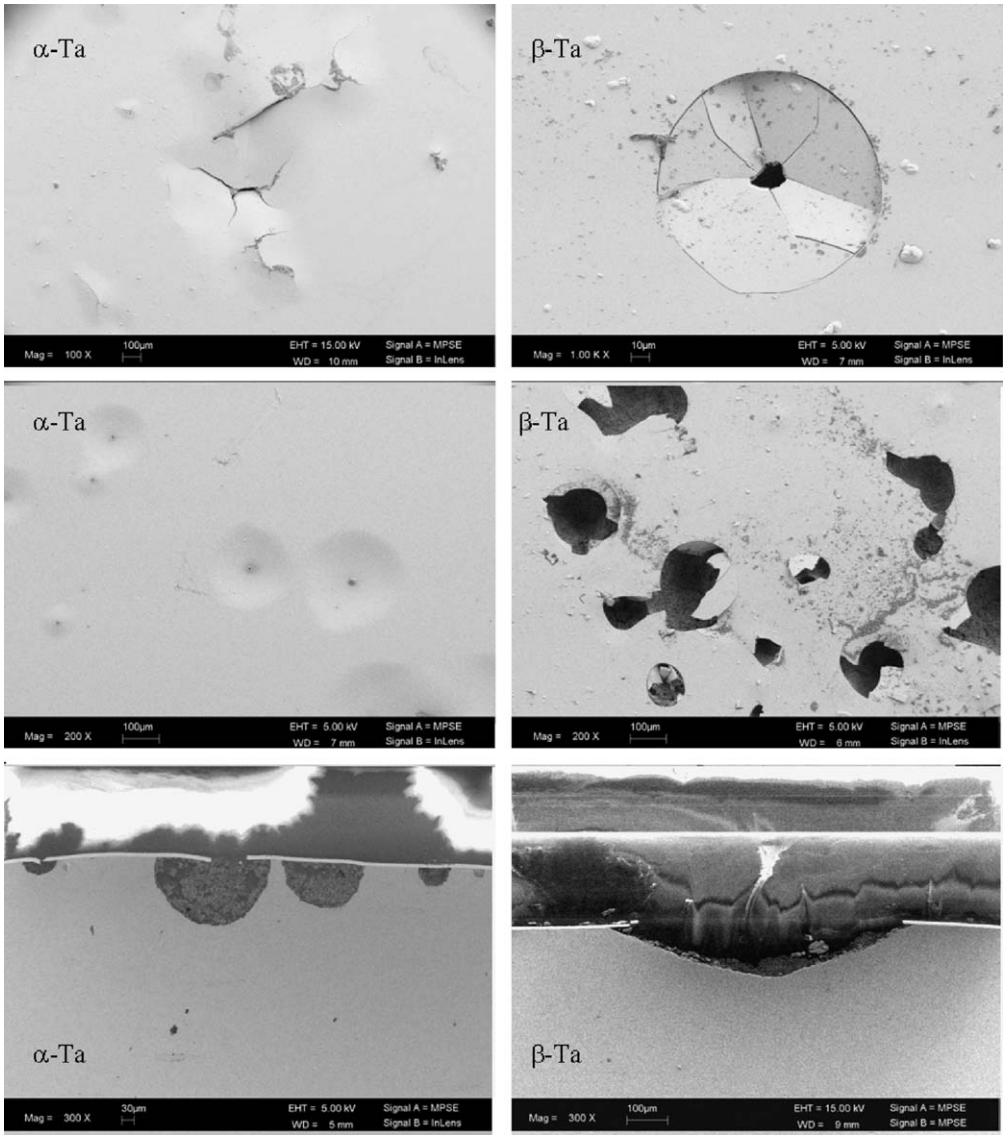

Fig. 7. SEM images of the surface and cross-sections of thin α- and β-Ta coatings after the EIS measurement.

zation resistance of the interface between Ta and the electrolyte, and for the α-Ta coating, the total resistance (R_{tot}) is the sum of the polarization resistance of the steel substrate through open pores (should any exist) and the resistance of the electrolyte in the Ta coating pores. The polarization resistance of Ta foil increases with increasing immersion time up to 4 h, and then remains constant over 4 days (Fig. 9). The increase in R_p may be due to passivation, which is confirmed by the increase in the open circuit potential as a function of time. For the 50 and 100 μm thick coatings, a decrease in R_{tot} in the early stages of immersion is observed, reflecting electrolyte penetration in the very fine pores [11].

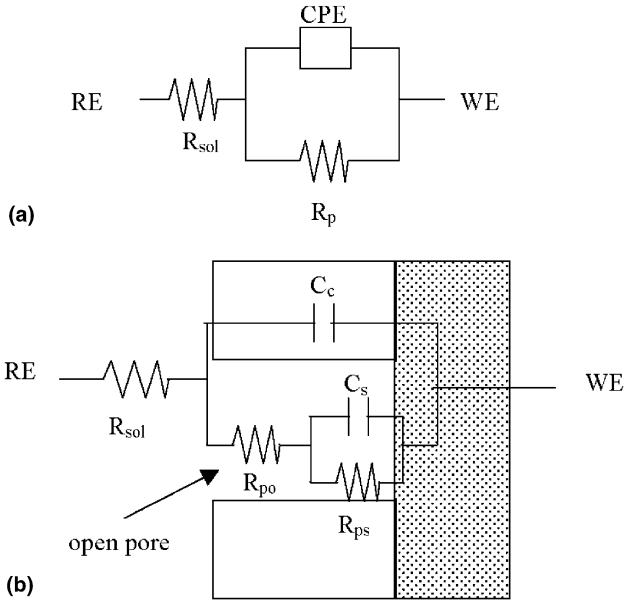

Fig. 8. Equivalent circuit models to fit experimental EIS data: (a) used for Ta foil and the 50 and 100 μm α-Ta coatings and (b) used for thin α- and β-Ta coatings. RE and WE represent reference electrode and working electrode, respectively.

However, no further decrease in R_{tot} of either 50 μm or 100 μm thick films is observed 8 h after immersion and R_{tot} becomes almost constant. Moreover EDX analysis showed no evidence of corrosion from the steel substrate through pores. The presence of open pores for such thick coatings is not therefore likely; nonetheless, impermeable and/or permeable pores may be important factors causing differences in the magnitude of R_{tot}. Additionally, duplicate samples of the same thickness produced under the same sputtering conditions revealed little variation in R_{tot} for a given thickness indicating that the formation and distribution of pores are random. Overall, α-Ta coatings of 50 μm or greater thickness behave like bulk Ta with respect to corrosion performance.

The EIS spectra of thin α- and β-Ta coatings were analyzed using the EC model (Fig. 8b) consisting of the polarization resistance (R_{ps}) and capacitance (C_s) of the steel substrate, the pore resistance (R_{po}), the coating capacitance (C_c), and the solution resistance (R_{sol}). The model represents localized corrosion of the steel substrate exposed to the electrolyte through permeable defects in the coating, such as open pores [11,20]. Here, the pore resistance to the ionic current provides information on degradation of the coating [23]. As thin α- and β-Ta coatings show two time constants in the EIS spectra (Fig. 6), the impedance Z at high frequency is represented by the parallel circuit (R_{po}, C_c), with a characteristic time constant τ_c that corresponds to the dielectric behaviour of the coatings. The active pits produced at open pores are described by the other parallel subcircuit (R_{ps}, C_s) with a second time constant τ_s, reflected in the low frequency part of the EIS spectra.

Based on the model, the evolution of pore resistance (R_{po}) and polarization resistance of the steel substrate (R_{ps}) through open pores is shown in Fig. 10. During initial exposure, the thicker β-Ta coating has a much greater R_{po} value than the thinner one, while there is

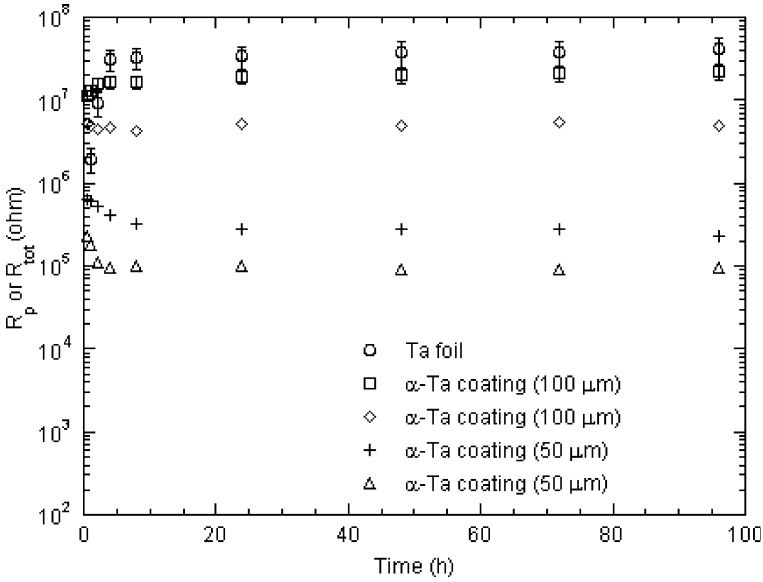

Fig. 9. R_p of Ta foil and R_{tot} of the 50 and 100 μm α-Ta coatings as a function of time. Error bars not visible are present within symbols.

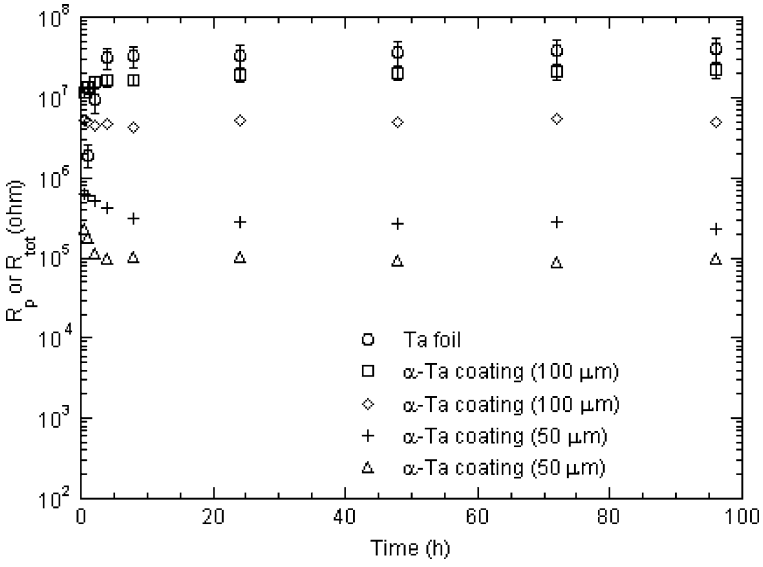

Fig. 10. R_{ps} and R_{po} of thin Ta coatings as a function of time. Error bars are within the symbols.

no significant difference between R_{po} values of α-Ta coatings with different thicknesses. These results suggest that the thin β-Ta coatings exhibit smaller voids than their α-Ta counterparts, resulting in decreased porosity of the former, as their thickness increases from 5 to 10 μm, due to void masking effects.

The continuous decreases in R_{po} and R_{ps} as a function of time are observed for both α- and β-Ta thin coatings. Specifically, the thin β-Ta coatings show a rapid decrease in R_p after 8 h for 5 μm and 24 h for 10 μm, while the thin α-Ta coatings undergo a gradual decrease in R_p during long exposure. The decrease in R_{po} is indicative of a change in pore size due to cracking and/or delamination of the coating, which is seen for thin β-Ta coatings (Fig. 7). In contrast large pinholes and cracks were observed in α-Ta coatings after corrosion. As mentioned earlier, the greater degree of delamination of the β-Ta coating over α—is attributed to the brittle nature of the β phase. Therefore, the α phase is preferred over β phase with respect to longer term corrosion performance. The reduction of R_{ps}, indicating an increase in the surface area of steel substrate exposed to electrolyte through open pores, may be related to (a) increasing open pore area with immersion time (change in R_{po}), or (b) increasing a surface area in steel under the pore, without significant change of the pore size (small or no change in R_{po}).

4. Conclusions

The corrosion behaviour of magnetron sputtered α- and β-Ta coatings as a function of thickness was evaluated electrochemically in a deaerated 0.5 M H_2SO_4 solution. Galvanic current measurements revealed that the current density linearly increases with an increasing ratio of cathodic (Ta) to anodic (AISI 4340 steel) area. In galvanic coupling, the contribution of the cathodic reaction was not significant. However, the galvanic measurements demonstrated that localized corrosion is accelerated by galvanic action when the steel substrate is exposed to the electrolyte through open micropores in the coating.

Polarization curves showed that the corrosion and passivation current densities of α-Ta and β-Ta coatings decreased significantly with increasing coating thickness. Furthermore, at 100 μm thickness, the polarization behaviour is equivalent to that of bulk Ta foil. The most important factor in corrosion of magnetron sputtered Ta coatings is the presence of defects such as pinholes and porosity formed during sputtering. Thus the overall corrosion process is dominated by local active dissolution of steel, which takes place as the substrate becomes exposed through open pores.

The impedance behaviour of thin α- and β-Ta coatings over long exposure times showed that the β-Ta coating is more susceptible to delamination due to its brittle nature; the α-phase is therefore preferred for protecting steel. In contrast to the thin Ta coatings, no significant degradation was observed in the α-Ta coatings of 50 and 100 μm thickness, where the electrochemical impedance behaviour was comparable to that of bulk Ta foil.

Acknowledgments

This work was conducted by NJIT as part of the Sustainable Green Manufacturing Program, through the National Defense Center for Environmental Excellence, contract DAAE30-98-C-1050.

References

[1] S.L. Lee, M. Cipollo, D. Windover, C. Rickard, Surf. Coat. Technol. 120/121 (1999) 44.
[2] S.L. Lee, D. Windover, M. Audino, D.W. Matson, E.D. McClanahan, Surf. Coat. Technol. 149 (2002) 62.

[3] L.A. Clevenger, A. Mutscheller, J.M.E. Harper, C. Cabral Jr., K. Barmak, J. Appl. Phys. 72 (1992) 4918.
[4] N. Schwartz, E.D. Feit, J. Electrochem. Soc. Solid State Sci. Technol. 124 (1977) 125.
[5] I.M. Notter, D.R. Gabe, Corros. Rev. 10 (1992) 217.
[6] B. Elsener, A. Rota, H. Böhni, Mater. Sci. Forum 44/45 (1989) 29.
[7] I.M. Notter, D.R. Gabe, Corros. Sci. 34 (1993) 851.
[8] W. Tato, D. Landolt, J. Electrochem. Soc. 145 (1998) 4173.
[9] H.A. Jehn, Surf. Coat. Technol. 125 (2000) 212.
[10] J. Creus, H. Mazille, H. Idrissi, Surf. Coat. Technol. 130 (2000) 224.
[11] C. Liu, Q. Bi, A. Leyland, A. Matthews, Corros. Sci. 45 (2003) 1257.
[12] L. Gladczuk, A. Patel, C. Singh Puar, M. Sosnowski, Thin Solid Films 467 (2004) 150.
[13] M. Pourbaix, Atlas of Electrochemical Equilibria in Aqueous Solutions, Pergamon Press, New York, 1966, p. 80.
[14] J.R. Macdonald, Impedance Spectroscopy, John Wiley & Sons, New York, 1987, p. 173.
[15] M.H. Read, D.H. Hensler, Thin Solid Films 10 (1972) 123.
[16] S. Lee, W. Ho, F.D. Lai, Mater. Chem. Phys. 43 (1996) 266.
[17] S.H. Ahn, J.H. Lee, J.G. Kim, J.G. Han, Surf. Coat. Technol. 177/178 (2004) 638.
[18] F. Mansfeld, Corrosion 27 (1971) 436.
[19] O. Kerrec, D. Devillier, H. Groult, M. Chemla, Electrochim. Acta 40 (1995) 719.
[20] D.K. Merl, P. Panjan, M. Cekada, M. Macek, Electrochim. Acta 49 (2004) 1527.
[21] F. Mansfeld, Electrochim. Acta 38 (1993) 1891.
[22] Q. Lu, S. Mato, P. Skeldon, G.E. Thompson, D. Masheder, Thin Solid Films 429 (2003) 238.
[23] M. Kendig, F. Mansfeld, S. Tsai, Corros. Sci. 23 (1983) 317.